

Localized Electrical Property Retrieval – Theories and Numerical Examples

Shao Ying Huang¹, Elfar Adalsteinsson², Berkin Bilgic², Shaohui Foong¹, and Lawrence L Wald³

¹Singapore University of Technology and Design, Singapore, Singapore, ²Massachusetts Institute of Technology, Cambridge, Massachusetts, United States, ³Massachusetts General Hospital, Charlestown, Massachusetts, United States

TARGETED AUDIENCE: Researchers desiring robust mapping of tissue electrical properties.

PURPOSE: Knowledge of the spatial distribution of electrical properties, namely dielectric constant, ϵ_r , and conductivity, σ , is valuable to various diagnostic and therapeutic technologies and for *in vivo* specific absorption rate (SAR) mapping in high-field magnetic resonance imaging (MRI). Mainly, two approaches have been proposed for MRI-based estimation of ϵ_r and σ ; electric properties tomography (EPT) [1,2] based on the integration version of the Maxwell's equations, and local Maxwell tomography (LMT) [3] based on the Maxwell's equations. EPT requires the absolute phase of B_1^+ and it works based the "half phase" assumption that $\varphi^+/2 = \varphi^-/2$ at 3T or below and requires a large integration volume for high accuracy [4]. LMT has no phase assumptions and it was proposed to work at 7T with multiple channels. In our work, we propose a new method to retrieve the electrical properties of tissues when the half phase assumption holds, termed Localized Electrical Property Retrieval (LEPR). For this method, only surface integration is needed rather than a volume one. Furthermore, the surface integrals can be chosen so that only B_1^+ or B_1^- is needed in the calculation, meaning it does not require the z -component of the magnetic field, which is similar to EPT. In this abstract, the theory of LEPR is presented in detail. For LEPR and EPT that both work for 3T or below, under the tested simulation data where ground-truth is known, the LEPR maps out-perform EPT. **METHODS:** The time

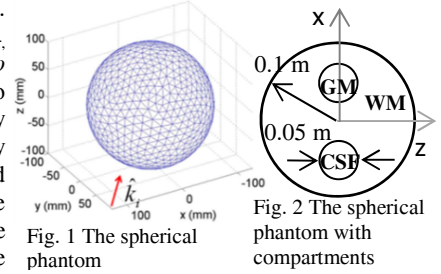


Fig. 1 The spherical phantom

Fig. 2 The spherical phantom with compartments

dependent magnetic flux density (called magnetic field in this context), $\vec{B}(\vec{r}, t) = \vec{B}(\vec{r}) e^{i\omega t}$, satisfies

- (1) dependent magnetic flux density (called magnetic field in this context), $\vec{B}(\vec{r}, t) = \vec{B}(\vec{r}) e^{i\omega t}$, satisfies
- (2) Maxwell's equations. Surface integrating both sides of Faraday's law (1) and applying Stoke's theorem to the left hand side gives (2), where A and ∂A are an area and the closed contour of that area, respectively. By line integrating the source free Ampere's law in (3) along a closed contour at each side of (3), we get to (4), where
- (3) $\nabla \times \vec{H}(\vec{r}) = i\omega \epsilon_c \vec{E}(\vec{r})$
- (4) $\epsilon_c = \epsilon_r - i\sigma/\omega$, ϵ_c is assumed to be constant along the integration contour. By substituting (2) into (4) and assuming that permeability is the same within the area of integration, the complex ϵ_c can be expressed using
- (5) In (5), the x -, y -, z -components of the magnetic field appear needed in the calculation. Stoke's theorem is

$$\nabla \times \vec{E}(\vec{r}) = -i\omega \vec{B}(\vec{r}) \quad (1)$$

$$\oint_{\partial A} \vec{E}(\vec{r}) \cdot d\vec{\ell} = -i\omega \int_A \vec{B}(\vec{r}) \cdot d\vec{a} \quad (2)$$

$$\nabla \times \vec{H}(\vec{r}) = i\omega \epsilon_c \vec{E}(\vec{r}) \quad (3)$$

$$\oint_{\partial A} \nabla \times \vec{H}(\vec{r}) \cdot d\vec{\ell} = i\omega \epsilon_c \int_A \vec{E}(\vec{r}) \cdot d\vec{\ell} \quad (4)$$

$$\epsilon_c = \oint_{\partial A} \nabla \times \vec{B}(\vec{r}) \cdot d\vec{\ell} / (\mu\omega^2 \int_A \vec{B}(\vec{r}) \cdot d\vec{a}) \quad (5)$$

applied to the numerator in (5), generating (6) with the recognition that $\nabla \cdot \vec{B}(\vec{r}) = 0$, (Gauss' law). Therefore, based on (6), if the integration area is in parallel to the z -direction, only B_x and B_y components are needed in the calculation. Equation (7) and (8) show the expressions for ϵ_c when the integration area is in parallel to the xz - and the yz -planes, respectively. If the data are acquired in a way that $dy = dx$, then $dydz = dx dz$ and $A_{xz} = A_{yz}$. Therefore, $dy = dx = d$ and $A_{xz} = A_{yz} = A$. Thus, ϵ_c can be expressed using B_1^+ as shown in (9), where A is the area on the xz - or yz -plane of a single voxel or of multiple voxels with certain excitations and objects. Equation (9) may be obtained by taking other derivation paths. A B_1^- version of (9) is derivable. The method is validated in a 3-compartment numerical spherical phantom (Fig. 1 and Fig. 2) comprising cerebrospinal fluid (CSF), white matter (WM), and grey matter (GM). SEMCAD based on FDTD is used for full-wave simulations. B_1^+ - and B_1^- - maps are calculated for the phantom at 128 MHz ($B_0 = 3T$). The ϵ_r and σ of the tissues at 128

$$\epsilon_c = \frac{\int_A \nabla \times \vec{B}(\vec{r}) \cdot d\vec{\ell}}{\mu\omega^2 \int_A \vec{B}(\vec{r}) \cdot d\vec{a}} = \frac{\int_A [\nabla \cdot (\vec{B}(\vec{r})) - \nabla^2 \vec{B}(\vec{r})] \cdot d\vec{a}}{\mu\omega^2 \int_A \vec{B}(\vec{r}) \cdot d\vec{a}} = \frac{-\int_A \nabla^2 \vec{B}(\vec{r}) \cdot d\vec{a}}{\mu\omega^2 \int_A \vec{B}(\vec{r}) \cdot d\vec{a}} \quad (6)$$

$$\epsilon_c = -\int_{A_{xz}} \nabla^2 B_y(\vec{r}) dx dz / \left(\mu\omega^2 \int_{A_{xz}} B_y(\vec{r}) dx dz \right) \quad (7)$$

$$\epsilon_c = -\int_{A_{yz}} \nabla^2 B_x(\vec{r}) dy dz / \left(\mu\omega^2 \int_{A_{yz}} B_x(\vec{r}) dy dz \right) \quad (8)$$

$$\epsilon_c = \frac{-\int_A \nabla^2 [B_x(\vec{r}) + iB_y(\vec{r})] da}{\mu\omega^2 \int_A [B_x(\vec{r}) + iB_y(\vec{r})] da} = \frac{-\int_A \nabla^2 B_1^+ da}{\mu\omega^2 \int_A B_1^+ da} \quad (9)$$

NRMSE = $\frac{100 \times \|M_{Retrieved} - M_{True}\|_2}{\|M_{True}\|_2}$ (10)

Table I Electrical Properties

Tissue	ϵ_r	σ (S/m)
CSF	84.0	2.1
WM	52.5	0.3
GM	73.5	0.6

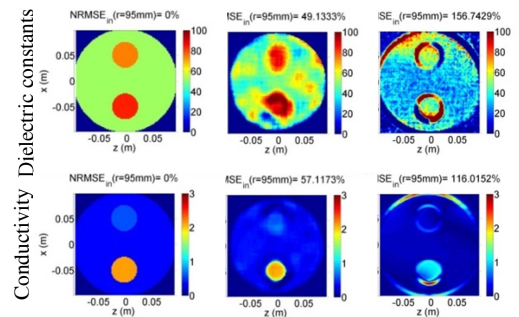
Table II Data Retrieval for a Single Voxel

	Voxel /pixel	ϵ_r	σ (S/m)	NRMSE	
				ϵ_r	σ
LEPR	1x1	51.87	0.34	1.3%	0.1%
	3x3x3	36.09	0.22	31.3%	36.0%
EPT	5x5x5	40.39	0.25	23.1%	27.4%

MHz are tabulated in Table I [5]. The background is air. The excitation source is a single planes wave (\hat{k}_i in Fig. 1). ϵ_r and σ are retrieved for a single voxel at the center of the sphere based on the B_1 data of different sizes from its neighborhood using LEPR and EPT. The half phase assumption is held. Moreover, ϵ_r - and σ -maps are obtained using different methods and compared. **RESULTS:** Table II shows the retrieved data for a single voxel using different size of B_1 data and the corresponding normalized root-mean-square error (NRMSE) by applying different methods. As can be seen in Table I, LEPR shows an NRMSE of 1.3% for ϵ_r and 0.2% for σ based on the calculation using data of a single voxel. For EPT, the NRMSE decreases as more voxels are used in the integration. Fig. 3 (a) - (c) show the true ϵ_r - and σ -maps, and the retrieved ones using LEPR and EPT, respectively. The signal to noise ratio (SNR) of the B_1 maps is 100. The 1st and 2nd rows show the ϵ_r - and σ -maps, respectively. The third order Savitsky-Golay (SG) smoothing filter with a window size of 7 in three directions around each voxel and median filtering were applied. The NRMSE's for the points within the sphere (radius = 95mm) are calculated using (10). NRMSEs arise from both tissue boundaries effects and the accuracy of the retrieval in the homogeneous area. **DISCUSSION:** Single voxel, noise-free performance is high for LEPR. As shown in Fig. 3, with SNR=100, the proposed method shows lower NRMSE for both ϵ_r and σ than EPT. The same smoothing filter is used. This indicates the accuracy of the retrievals and the smaller area of inaccuracy at the tissue boundaries using LEPR. It also implies the smaller sensitivity of LEPR to noise.

CONCLUSION: The proposed Localized Electrical Property Retrieval provides an alternative to retrieve electrical properties of tissues using only a single B_1 -map. It reduces the inaccurate area near the tissue boundaries with B_1 maps of the same resolution and appears accurate down to a single voxel, subject to SNR constraints.

REFERENCES: [1] Katscher U et al, IEEE Trans Med Imaging 2009; 28:1365. [2] Voigt T Magn Reson in Med 2011; 66:456. [3] Sodickson D K ISMRM 2012, 387 [4] S. Jaewook, ISMRM 2012 2533 [5] <http://niremf.ifac.cnr.it/tissprop>



(a) True maps (b) LEPR (c) EPT
Fig.3. True maps and the retrieved electrical property maps on $y = 0$ xz -planes